



HAL
open science

USE OF A PARAMETRIC FINITE-ELEMENT MODEL OF THE MITRAL VALVE TO ASSESS HEALTHY AND PATHOLOGICAL VALVE BEHAVIORS

Alleau Thibaut, Laurent Lanquetin, Anne-Virginie Salsac

► **To cite this version:**

Alleau Thibaut, Laurent Lanquetin, Anne-Virginie Salsac. USE OF A PARAMETRIC FINITE-ELEMENT MODEL OF THE MITRAL VALVE TO ASSESS HEALTHY AND PATHOLOGICAL VALVE BEHAVIORS. ECCOMAS-MSF, 2019, 4th edition, Sep 2019, Sarajevo, France. hal-02491319

HAL Id: hal-02491319

<https://utc.hal.science/hal-02491319v1>

Submitted on 26 Feb 2020

HAL is a multi-disciplinary open access archive for the deposit and dissemination of scientific research documents, whether they are published or not. The documents may come from teaching and research institutions in France or abroad, or from public or private research centers.

L'archive ouverte pluridisciplinaire **HAL**, est destinée au dépôt et à la diffusion de documents scientifiques de niveau recherche, publiés ou non, émanant des établissements d'enseignement et de recherche français ou étrangers, des laboratoires publics ou privés.

USE OF A PARAMETRIC FINITE-ELEMENT MODEL OF THE MITRAL VALVE TO ASSESS HEALTHY AND PATHOLOGICAL VALVE BEHAVIORS

Alleau Thibaut ^{1,2}, Anne-Virginie Salsac ¹, Laurent Lanquetin ²

¹ Biomechanics and Bioengineering Laboratory (UMR 7338), Université de Technologie de Compiègne - CNRS, Alliance Sorbonne Université, Compiègne (France)

² Segula Matra Automotive, Trappes (France)

thibaut.alleau@utc.fr, laurent.lanquetin@segula.fr, a.salsac@utc.fr

Abstract

The present study is focused on the mitral heart valve, which is the valve that separates the left ventricle from the left atrium. The aim is to provide a parametrical geometrical model of the valve in order to study pathological valves (e.g. suffering from cord rupture) and compare it to the physiological case. A finite element model is used to quantify how the valve defects affect the valve dynamics during closure, the internal stress distribution along the valve leaflets and the level of regurgitation.

1. Introduction

The mitral valve is a cardiac valve composed of four elements: the anterior and posterior leaflets, the annulus which is the structure through which the leaflets are attached to the heart muscle, the chordae tendinae which are attached to pillars in the ventricular wall and ensure that the very flexible leaflets remain within the ventricle, the papillary muscles which are located at the tip of the chordae tendinae and actively modify the tension acting on the leaflets. These four elements allow a healthy mitral valve to let blood flow from the atrium to the ventricle during diastole, and to create a hermetic seal between the two chambers during systole. This seal prevents blood from regurgitating into the left atrium when being ejected from the ventricle. Several pathologies may exist, since each of the four elements (e.g. chordae rupture) may potentially be the source of dysfunctions. Mitral insufficiency is the most frequent valvular pathology in Western countries after aortic narrowing upon calcification [12].

Mitral valve scans obtained by magnetic resonance imaging, computed-tomography (CT-scan) or echocardiography [13, 8, 2, 14] can be used in computational analysis to have a better understanding of the valve function and help surgeons determine patient-specific medical treatments. It is, however, difficult to extrapolate results from one patient to another. Indeed, anatomical studies have shown that human mitral valve measures differ among patients [4, 10], but some patterns, however, exist [3, 5]. Another approach is thus to define the valve using a simplified parametric geometry. The advantage of such models is that one can vary the characteristic lengths of the valve systematically and simulate pathological conditions. Several geometrical valve models have been developed in the literature [7, 6, 11], but pathological conditions have been little studied. The aim of the present study is to develop a geometrical model of mitral valves in both healthy and pathological states.

2. Material and methods

2.1. Mitral valve definition

We create a parametric model of a valve with a left-to-right symmetry using FreeCAD and Fortran subroutines (Figure 1a). It is constructed by defining points along the edge of the leaflets and using

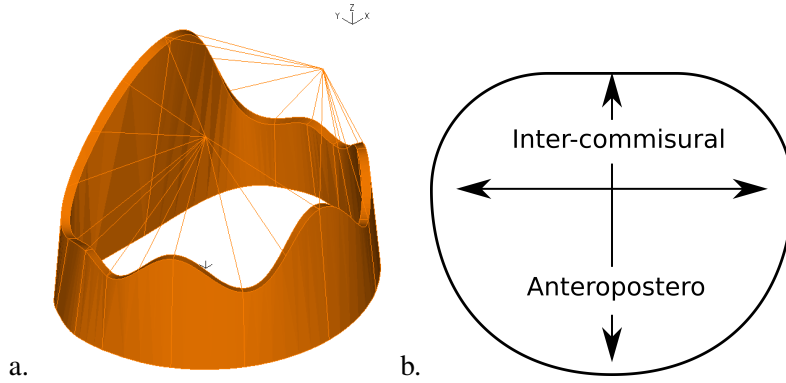


Figure 1: Parametric geometrical model of mitral valve. a. Three-dimensional representation of the modeled valve. b. Geometrical definition of the mitral annulus.

b-splines to reconstruct their contour. The posterior (respectively, anterior) leaflet is inclined by an angle of 5.3° (respectively, 8.3°). Their height ranges from 7.7 mm to 23.4 mm. The thickness is uniform and equal to 0.8 mm.

The annulus of the mitral valve is defined using a planar D-shape with a ratio $3/4$ between the anteropostero and the inter-commisural diameters (Figure 1b), similarly to the Carpentier-Edwards Physio annuloplasty ring (Edwards Lifesciences). The annulus is supposed to be planar and the anteropostero diameter to be 3 cm.

The papillary muscles tips, onto which the chordae tendineae are attached, are placed at fixed positions obtained from medical data [10]. The chordae tendineae are represented as cords going from the papillary muscle tips to the border of the leaflets. Their distribution is approximately uniform along the leaflet edges.

The geometric model of the valve is exported as an IGES file. Specific python macros are used to make adjustments on the FreeCAD model, for instance to create the b-splines and isolate points along the b-splines.

2.2. Model of the mitral function

The closure of the mitral valve is simulated using a finite element method (software ADINA v9.4), modeling the displacement of the leaflets under a hydrodynamic pressure. Being little influenced by fluid-structure interactions, the valve closure can be well approximated by structure-only simulations. The leaflets are loaded under a pressure ramp corresponding to the systolic pressure evolution. The pressure ramp start at 0 s and reach its peak value at 0.1 s.

The annulus and the papillary muscle tips are fixed during computation. The leaflet material is assumed to be isotropic linear elastic, with Young modulus $E = 3$ MPa, Poisson ratio $\nu = 0.45$ and density $\rho = 1$ kg.m⁻³. The chordae tendineae are also supposed to be isotropic linear elastic but with Young modulus $E = 40$ MPa.

We assume large displacement and use a second-order implicit time integration scheme called Bathe scheme ([1, 9]). An implicit contact method is used, setting the compliance factor of the constraint function to 1×10^{-9} . Double-sided detection is activated on all the surfaces of the leaflets.

The leaflets are discretized using 4227 elements (27-node hexahedrons and 11-node tetrahedrons) of maximum length 8×10^{-1} mm. The chordae tendineae are discretized using 457 2-node truss elements. A time step of 1×10^{-4} s is used from 0 s to 0.1 s and of 1×10^{-2} s hereafter until the end of the computation. In addition, an adaptative time step method is used if convergence difficulties arise, possibly reducing the time step to 1×10^{-7} s and 1×10^{-5} s, respectively. The linear part of the problem is solved directly using *LU* decomposition, and the non-linear part using the Newton-Raphson algorithm with a maximum of 15 iterations.

The pathological case shown was obtained by rupturing the chordae tendineae, attached to the anterior leaflet. This was modeled by deleting the corresponding elements in the numerical model.

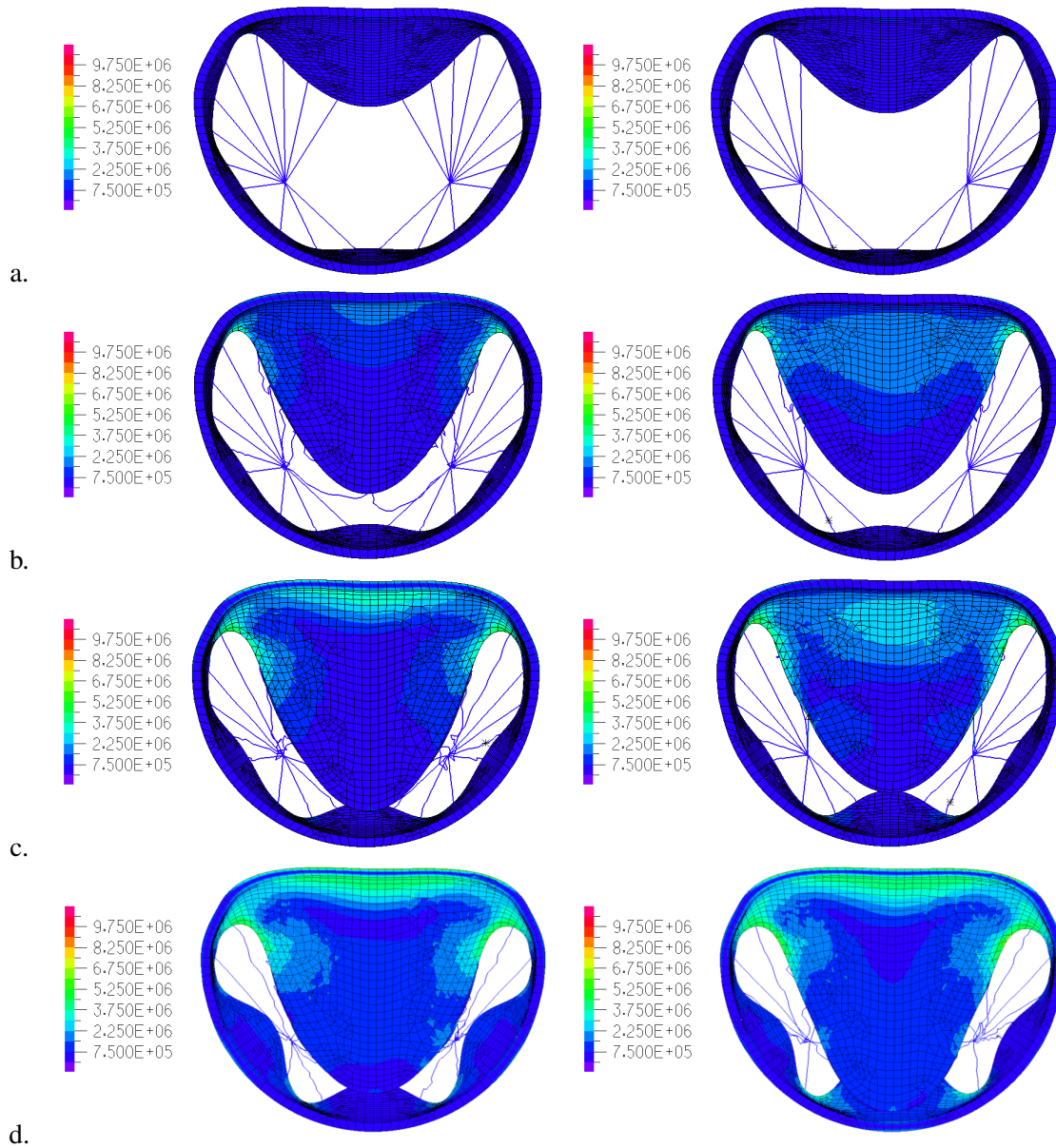


Figure 2: Stress distribution within the leaflet of the mitral valve during closure at times $t = 0.01$ s (a), 0.03 s (b), 0.05 s (c) and 0.09 s (d). Left column: healthy valve, right column: pathological valve. The units are in dyne.cm^{-2} ($1 \text{ dyne.cm}^{-2} = 0.1 \text{ Pa}$)

3. Results

The stress distribution is shown in Figure 2 during valve closure. Even though the stress field remains of the same magnitude in the pathological and healthy cases, differences in distribution are observed in the center of the anterior leaflet and close to the clefts of the posterior leaflet. The orifice area projected within the annular plane is larger in the pathological case than in the healthy case. Cord rupture will indeed cause regurgitation during diastole. The lack of chordae tendineae in the pathological case also implies a larger amplitude of the anterior leaflet motion, as it is less attached to the papillary muscle than in the healthy anterior leaflet. At $t = 0.09$ s, the pathological anterior leaflet is nearly above the annular plane. We thus observe a mitral valve prolapse.

4. Conclusion

We have built a geometrical model of the mitral valve capable of modeling both healthy and pathological mitral valves. The parameters allow to test several mitral valves, and to assess in each case the mitral valve function using a finite element method. The model might be of use to numerically test medical procedure on mitral valves.

References

- [1] K.-J. Bathe and G. Noh. *Insight into an implicit time integration scheme for structural dynamics*, Computers & Structures, 98-99:1–6, 2012.
- [2] C. Chnafa, S. Mendez, and F. Nicoud. *Image-based large-eddy simulation in a realistic left heart*, Computer & Fluids, 94:173–187, 2014.
- [3] A. Drach, A. H. Khalighi, F. M. ter Huurne, et al. *Population-averaged geometric model of mitral valve from patient-specific imaging data*, Journal of Medical Devices, 9:030952, 2015.
- [4] S. Gunnal, M. Farooqui, and R. Wabale. *Study of mitral valve in human cadaveric hearts*, Heart Views, 13:132, 2012.
- [5] A. H. Khalighi, A. Drach, C. H. Bloodworth, et al. *Mitral valve chordae tendineae: topological and geometrical characterization*, Annals of Biomedical Engineering, 45:378–393, 2016.
- [6] K. S. Kunzelman, D. Einstein, and R. Cochran. *Fluid-structure interaction models of the mitral valve: function in normal and pathological states*, Philos. Trans. R. Soc. London, Ser. B, 362:1393–1406, 2007.
- [7] K. D. Lau, V. Diaz, P. Scambler, et al. *Mitral valve dynamics in structural and fluid-structure interaction models*, Medical Engineering & Physics, 32:1057–1064, 2010.
- [8] X. Ma, H. Gao, B. E. Griffith, et al. *Image-based fluid–structure interaction model of the human mitral valve*, Computers & Fluids, 71:417–425, 2013.
- [9] G. Noh, S. Ham, and K.-J. Bathe. *Performance of an implicit time integration scheme in the analysis of wave propagations*, Computers & Structures, 123:93–105, 2013.
- [10] T. Sakai, Y. Okita, Y. Ueda, et al. *Distance between mitral anulus and papillary muscles: anatomic study in normal human hearts*, J. Thorac. & Cardio. Sur. 118:636–641, 1999.
- [11] X. Shen, T. Wang, X. Cao, et al. *The geometric model of the human mitral valve*, PLOS ONE, 12:e0183362, 2017. D. Zhang, editor.
- [12] J. P. Singh, J. C. Evans, D. Levy, et al. *Prevalence and clinical determinants of mitral, tricuspid, and aortic regurgitation (the framingham heart study)*, Am. J. Cardiol. 83:897–902, 1999.
- [13] M. Toma, D. R. Einstein, C. H. Bloodworth, et al. *Fluid-structure interaction and structural analyses using a comprehensive mitral valve model with 3d chordal structure*, Int. J. Numer. Methods Biomed. Eng, 33:e2815, 2016.
- [14] E. Votta, E. Caiani, F. Veronesi, et al. *Mitral valve finite-element modelling from ultrasound data: a pilot study for a new approach to understand mitral function and clinical scenarios*, Philos. Trans. R. Soc. London, Ser. A, 366:3411–3434, 2008.